

Coupled cluster calculations of optical rotatory dispersion of (*S*)-methyloxirane

Mary C. Tam, Nicholas J. Russ, and T. Daniel Crawford^{a)}

Department of Chemistry, Virginia Tech, Blacksburg, Virginia 24061

(Received 19 April 2004; accepted 20 May 2004)

Coupled cluster (CC) and density-functional theory (DFT) calculations of optical rotation, $[\alpha]_{\lambda}$, have been carried out for the difficult case of (*S*)-methyloxirane for comparison to recently published gas-phase cavity ringdown polarimetry data. Both theoretical methods are exquisitely sensitive to the choice of one-electron basis set, and diffuse functions have a particularly large impact on the computed values of $[\alpha]_{\lambda}$. Furthermore, both methods show a surprising sensitivity to the choice of optimized geometry, with $[\alpha]_{355}$ values varying by as much as $15 \text{ deg dm}^{-1} (\text{g/mL})^{-1}$ among molecular structures that differ only negligibly. Although at first glance the DFT/B3LYP values of $[\alpha]_{355}$ appear to be superior to those from CC theory, the success of DFT in this case appears to stem from a significant underestimation of the lowest (Rydberg) excitation energy in methyloxirane, resulting in a shift of the first-order pole in $[\alpha]_{\lambda}$ (the Cotton effect) towards the experimentally chosen incident radiation lines. This leads to a fortuitous positive shift in the value of $[\alpha]_{355}$ towards the experimental result. The coupled cluster singles and doubles model, on the other hand, correctly predicts the position of the absorption pole (to within 0.05 eV of the experimental result), but fails to describe correctly the shape/curvature of the ORD region $\lambda=355$, resulting in an incorrect prediction of both the magnitude and the *sign* of the optical rotation.

© 2004 American Institute of Physics. [DOI: 10.1063/1.1772352]

I. INTRODUCTION

A long-standing problem in natural products chemistry is the determination of the absolute configuration of newly isolated compounds. Although the assessment of the enantiomeric purity of such chiral species is routinely achieved by measuring optical rotation angles or integrating chiral GC/HPLC traces, determining the absolute configuration is more difficult.^{1,2} The most convincing analyses rely on x-ray crystallographic data of the compound itself (using anomalous dispersion) or of a derivative that incorporates a known stereocenter. In the case of a noncrystalline compound, asymmetric synthesis, or total synthesis from starting materials of known absolute configuration, must be performed. When these methods fail, less secure chiroptical and NMR methods are used. All of these approaches are time consuming, and none are guaranteed to be successful.

An alternative approach is to compute directly the chiroptical properties of selected molecular structures and compare the results with the associated properties [optical rotation angles, optical rotatory dispersion (ORD) spectra, or circular dichroism (CD) spectra] of the original natural product isolate.³⁻⁹ The quantum mechanical foundation for such computations has been known since the work of Rosenfeld in 1928.¹⁰ Using time-dependent perturbation theory, one may show that the angle of rotation, $[\alpha]_{\omega}$, of plane-polarized light of frequency ω in a chiral medium is related to the trace of the frequency-dependent electric-dipole magnetic-dipole polarizability tensor:

$$\beta(\omega) = \frac{c}{3\pi h} \text{Im} \sum_{n \neq 0} \frac{\langle 0 | \boldsymbol{\mu} | n \rangle \langle n | \mathbf{m} | 0 \rangle}{\omega_{n0}^2 - \omega^2}, \quad (1)$$

where $\boldsymbol{\mu}$ and \mathbf{m} are the electric and magnetic dipole operators, respectively, and the summation runs over excited electronic (unperturbed) wave functions, $|n\rangle$. This tack has been taken with both semiempirical¹¹⁻¹³ and *ab initio* quantum chemical techniques,^{4,14-16} most recently with density functional theory^{6,8,17,18} and coupled cluster theory¹⁹⁻²¹ and several applications have appeared in the literature.^{5,9,22-29} Unfortunately, the quality of such theoretical predictions is often difficult to assess because fair comparisons with experimental data are not straightforward. First, the theoretical approach may contain many sources of error, such as choice of one-electron basis set, dynamic electron correlation effects, etc. Second, experimental data are often obtained under widely varying conditions, and solvent and/or temperature effects, as well as conformational averaging, may have a significant impact on measured chiroptical spectra.

A recent breakthrough in the development of cavity ringdown polarimetry (CRDP) by Müller, Wiberg, and Vaccaro has allowed ultrasensitive gas-phase measurements of optical rotation of a number of small chiral molecules, thus opening the door to more systematic comparisons between theory and experiment.^{30,31} Müller *et al.* reported that, contrary to conventional wisdom, solvent effects can indeed be significant, perhaps leading to dramatic differences in both magnitude and sign of optical rotation angles relative to gas-phase results. For example, among the molecules studied by Müller *et al.* is propylene oxide (also known as methyloxirane), a potentially ideal test case for higher-level theoretical models

^{a)}Electronic mail: crawdad@vt.edu

because it is conformationally rigid and contains only four nonhydrogen atoms. Müller *et al.* measured a 355 nm specific rotation of the (S) enantiomer of methyloxirane of $+10.2 \text{ deg dm}^{-1} (\text{g/mL})^{-1}$ in the gas phase and $-26.4 \text{ deg dm}^{-1} (\text{g/mL})^{-1}$ in cyclohexane. These results agree qualitatively with those of Kumata *et al.*, who reported a wide variation of sodium D-line (589 nm) specific rotation of (S)-methyloxirane in benzene [$-30.6 \text{ deg dm}^{-1} (\text{g/mL})^{-1}$] versus water [$(+4.3 \text{ deg dm}^{-1} (\text{g/mL})^{-1})$].³²

In the only theoretical comparison to these new experimental results to date, Giorgio *et al.* recently reported density-functional theory (DFT) specific rotation data for (S)-methyloxirane using a variety of basis sets.³³ They found that the B3LYP functional was capable of predicting the correct sign for the optical rotation with the use of high-angular-momentum correlation-consistent basis sets³⁴ or specially tailored Sadlej basis sets,^{35,36} but the magnitude of the rotation was overestimated by a factor of two. In addition, they reported that large-basis-set Hartree–Fock optical rotation calculations disagreed qualitatively with the results of Müller *et al.*, a point recently made in several systematic studies by Cheeseman *et al.*^{6,8} Giorgio *et al.* also indicated that the anomalously large frequency dispersion observed in (S)-methyloxirane is related to the lowest energy Cotton effect, even though the corresponding absorption occurs at only 174.1 nm (7.12 eV)³⁷ some distance from the wavelength of the CRDP radiation source at 355 nm (3.49 eV) used by Müller and co-workers.³¹

Given the apparent need for higher-level theoretical calculations of optical rotation in (S)-methyloxirane, we have applied coupled cluster linear response theory to this problem. Coupled cluster is widely regarded as the most reliable quantum chemical approach for computing a variety of properties of small molecules, including molecular structure, vibrational spectra, NMR chemical shieldings, UV/Vis spectra, and thermochemical properties.^{38–41} Thus, we seek to extend its applicability to optical rotation and to benchmark its accuracy relative to experiment. In particular, using a new implementation of the coupled cluster singles and doubles (CCSD) model for frequency-dependent properties, described in Sec. II we have considered the effect of basis set, optimized geometry, and gauge origin on the computed rotation angles of (S)-methyloxirane for comparison to both DFT data and the experimental results of Müller and co-workers. We find that: (1) the quality of both the DFT and coupled cluster predictions vary widely with basis set and choice of optimized structure; (2) DFT benefits from an incorrect prediction of the lowest energy Rydberg transition in methyloxirane; and (3) coupled cluster, while correct in its determination of the energy of the lowest Rydberg state, instead fails to predict the width of the pole surrounding the resonance.

II. COUPLED CLUSTER RESPONSE THEORY FOR OPTICAL ROTATION

The Rosenfeld β tensor in Eq. (1) may be computed within the coupled cluster model using response theory,^{42–46} in which β is related to the linear response function:

$$\beta(\omega) = \langle\langle \boldsymbol{\mu}; \mathbf{m} \rangle\rangle_{\omega} = \frac{d^2 \{L_{CC}\}_T}{d\boldsymbol{\mu} d\mathbf{m}}, \quad (2)$$

where $\{L_{CC}\}_T$ represents the time-averaged coupled cluster Lagrangian.⁴⁵ Evaluating the derivative above leads to an operator form of the linear response function:

$$\begin{aligned} \langle\langle \boldsymbol{\mu}; \mathbf{m} \rangle\rangle_{\omega} = & \frac{1}{2} \hat{C}^{\pm\omega} \hat{P}[\boldsymbol{\mu}(-\omega), \mathbf{m}(\omega)] [\langle 0 | \hat{\Lambda}[\bar{\boldsymbol{\mu}}, \hat{X}_{\mathbf{m}}^{\omega}] | 0 \rangle \\ & + \frac{1}{2} \langle 0 | \hat{\Lambda}[[\bar{H}, \hat{X}_{\boldsymbol{\mu}}^{\omega}], \hat{X}_{\mathbf{m}}^{-\omega}] | 0 \rangle], \end{aligned} \quad (3)$$

where $|0\rangle$ is the Hartree–Fock reference state, the overbar denotes the similarity transformation of the given operator [e.g., $\bar{H} = \exp(-\hat{T})\hat{H}\exp(\hat{T})$], and $\hat{\Lambda}$ is a cluster operator parametrizing the coupled cluster “left-hand” ground-state wave function (developed also in coupled cluster analytic energy gradient theory).^{47–51} The permutation operator $\hat{C}^{\pm\omega}$ simultaneously changes signs on the chosen field frequency, ω , and takes the complex conjugate of the equation, while $\hat{P}(\hat{A}, \hat{B})$ permuted the property operators \hat{A} and \hat{B} . The perturbed wave functions, $\hat{X}_{\boldsymbol{\mu}}^{\omega}$, are determined by solving the system of linear equations:

$$\langle \Phi_i | (\bar{H} - \omega) | \Phi_j \rangle \langle \Phi_j | \hat{X}_{\boldsymbol{\mu}}^{\omega} | 0 \rangle = -\langle \Phi_i | \bar{\boldsymbol{\mu}} | 0 \rangle, \quad (4)$$

where the Φ_i represents excited determinants. It is worth noting that the eigenvalues of the response matrix on the left-hand side of the above equation (sometimes referred to in the literature as the coupled cluster Jacobian matrix) are related to the excitation energies of the system, an approach to UV/Vis spectra known as the equation-of-motion coupled cluster (EOM-CC) method.^{43,52}

One may therefore evaluate the above linear response function by the following steps:

- (1) Solve the ground-state coupled cluster equations for the cluster operators, \hat{T} .^{53,54}
- (2) Compute the similarity transforms of the Hamiltonian, \bar{H} , and other operators required for the response function, i.e., $\bar{\boldsymbol{\mu}}$ and $\bar{\mathbf{m}}$.⁵²
- (3) Solve the left-hand ground-state wave function equations for $\hat{\Lambda}$.⁵¹
- (4) Solve the system of linear equations in Eq. (4) for each component of each perturbation for both positive and negative values of the field frequency, ω . For the optical rotation function, this leads to twelve sets of perturbed wave function equations which must be solved.
- (5) Compute the contributions to the total linear response function given in Eq. (3).^{43,46}

We have derived and implemented the linear response function for the Rosenfeld β tensor at the coupled-cluster singles and doubles (CCSD) level of theory within the program package PSI3.⁵⁵ We have adopted a factorization strategy of the many diagrams appearing implicitly in Eqs. (3) and (4) similar to that used in efficient ground-state coupled cluster energy and analytic gradient implementations, such that no single term scales worse than $\mathcal{O}(N^6)$.^{56,57} The pro-

gram makes full use of Abelian point-group symmetry when available for efficiency, though for (*S*)-methyloxirane, no such symmetry is present.

An important failing of the above approach to coupled cluster frequency-dependent properties, as noted by Pedersen and Koch,^{21,58–60} is its lack of origin independence for magnetic-field-dependent properties, such as optical rotation. Although this problem can be circumvented for Hartree–Fock and DFT response methods using gauge-including atomic orbitals (GIAOs, also known as London orbitals),^{6,15,61–63} this technique will not ensure origin invariance for conventional coupled cluster or perturbation methods due their lack of orbital optimization. On the other hand, GIAOs can substantially improve the basis-set dependence of magnetic-field dependent properties,⁶⁴ a point we will address below.

III. COMPUTATIONAL DETAILS

The optimized geometry of (*S*)-methyloxirane was determined using analytic energy gradients at the B3LYP^{65–67} and CCSD(T)^{50,53,68–71} levels of theory with two different basis sets: the standard 6-31G* split-valence basis set of Pople *et al.*⁷² and the correlation-consistent triple-zeta (cc-pVTZ) basis set of Dunning.³⁴ These four optimized structures were confirmed to be minima on the potential energy surface *via* harmonic vibrational frequency calculations, carried out using analytic energy second derivative methods.^{73,74}

Optical rotation calculations for a variety of wavelengths were carried out using the coupled cluster singles and doubles (CCSD) linear response approach described in the previous section and using time-dependent density-functional theory (TDDFT) with the B3LYP functional.^{5,6} The molecular center of mass was chosen as the origin for most of the calculations reported here, though the coordinates of the oxygen atom were used for additional analysis. The B3LYP data were obtained both with and without GIAOs for comparison to the CCSD results (*vide supra*). In addition, the positions of poles in the values of $[\alpha]$ (i.e., excitation energies) were computed using EOM-CCSD⁵² and TDDFT/B3LYP approaches.^{75,76}

In addition, several different basis sets were employed for the optical rotation calculations: (1) the split-valence basis sets, 6-31G*, 6-31++G**, and 6-311++G(2d,2p);⁷² (2) the correlation-consistent basis sets, cc-pVDZ, cc-pVTZ, aug-cc-pVDZ, d-aug-cc-pVDZ, and a mixed basis consisting of the aug-cc-pVTZ basis for carbon and oxygen and the aug-cc-pVDZ basis for hydrogen (238 contracted Gaussian functions);^{34,77,78} and (3) the Sadlej-pVTZ basis set, which was developed specifically for computations of electric properties, including dipole polarizabilities.^{35,36} Pure angular momentum polarization functions were used for the 6-311++G(2d,2p), correlation consistent, and Sadlej basis sets, while Cartesian polarization functions were used with all other basis sets. All electrons were correlated for the geometry and frequency calculations, but the core electrons were held frozen for all of the CCSD optical rotation and excitation energy calculations. (The only reason for this choice is a program limitation in the ACESII system, which was used for the structural optimizations. Coupled cluster geometries determined using frozen core orbitals differ negligibly—at

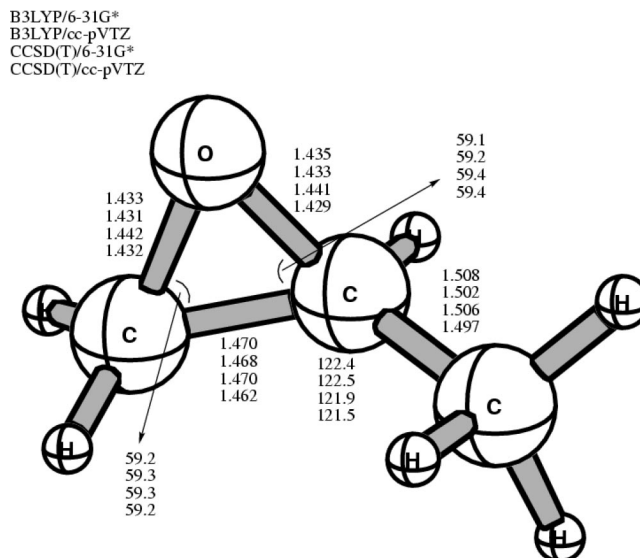


FIG. 1. Optimized geometries of (*S*)-methyloxirane using B3LYP and CCSD(T) methods with the 6-31G* and cc-pVTZ basis sets. Bond lengths are given in angstroms and bond angles in degrees.

most 0.001 Å in bond lengths and less than 0.1 degrees in bond and dihedral angles at the CCSD(T)/6-31G* level from the all-electron data used here.) Basis sets were obtained from the Extensible Computational Chemistry Environment Basis Set Database.⁷⁹

All coupled cluster optical rotation calculations were carried out with the PSI3 program package,⁵⁵ while B3LYP optical rotation calculations were carried out using GAUSSIAN 03.⁸⁰ Coupled cluster geometry optimizations, harmonic vibrational frequency calculations, and excitation energy calculations were carried out with the ACESII program package,⁸¹ while B3LYP optimized geometries, harmonic vibrational frequencies, and excitation energies were computed with the Gaussian suite.⁸⁰

IV. RESULTS AND DISCUSSION

Figure 1 reports the optimized geometry of (*S*)-methyloxirane at the B3LYP/6-31G*, B3LYP/cc-pVTZ, CCSD(T)/6-31G*, and CCSD(T)/cc-pVTZ levels of theory. Although the CCSD(T)/cc-pVTZ results are reasonably expected to be the most accurate, the rigid structure of this molecule depends very little on the choice of method, and all four structures agree very well with the experimentally inferred geometry of Creswell and Schwendeman.⁸² Bond lengths vary among the four methods only slightly (all within ~0.01 Å) and the variation in the bond angles is, at most, a few tenths of a degree. Most importantly, the angle of the methyl group out of the plane formed by the oxirane ring, which one might expect to be the most important structural feature influencing the computed rotations,^{16,27} varies by less than a degree (54.95 degrees at the B3LYP/cc-pVTZ level vs 55.89 degrees at the CCSD(T)/cc-pVTZ level). Nevertheless, as we show below, the choice of optimized structure still has a significant impact on the computed optical rotation.

Tables I and II report the computed values of $[\alpha]_{\lambda}$ [in deg dm⁻¹ (g/mL)⁻¹] at the B3LYP and CCSD levels of

TABLE I. B3LYP and CCSD specific rotation [$\text{deg dm}^{-1} (\text{g/mL})^{-1}$] for (S)-methyloxirane computed with various basis sets and optimized geometries at 589 nm. The center of mass is chosen to be the gauge origin.

Geometry type	6-31G*	6-31++G**	6-311++G(2d,2p)	cc-pVDZ	cc-pVTZ	aug-cc-pVDZ	d-aug-cc-pVDZ	mixed-cc-pVTZ ^a	aug-cc-pVTZ	Sadlej-pVTZ
B3LYP (GIAO)										
B3LYP/6-31G*	-22.6	-37.0	-14.9	-49.5	-24.5	-19.4	-11.8	-14.56	-12.7	-1.27
B3LYP/cc-pVTZ	-23.8	-37.0	-13.1	-49.0	-23.3	-16.8	-9.26	-11.93	-10.0	2.17
CCSD(T)/6-31G*	-27.8	-38.7	-16.7	-53.9	-27.5	-21.0	-12.9	-16.49	-14.2	-3.02
CCSD(T)/cc-pVTZ	-30.4	-38.8	-14.2	-55.2	-26.7	-18.1	-9.07	-13.47	-11.1	0.58
B3LYP (non-GIAO)										
B3LYP/6-31G*	-29.3	-36.0	-3.83	-44.8	-28.1	-21.0	-9.19	-11.56	-11.3	-10.4
B3LYP/cc-pVTZ	-28.1	-34.0	-1.94	-44.1	-27.4	-18.5	-6.58	-8.70	-8.49	-7.45
CCSD(T)/6-31G*	-33.9	-37.2	-5.28	-48.9	-31.6	-22.6	-10.8	-13.14	-12.0	-12.0
CCSD(T)/cc-pVTZ	-34.6	-34.8	-2.63	-49.7	-30.5	-19.5	-7.70	-9.74	-9.49	-8.69
CCSD										
B3LYP/6-31G*	-24.1	-49.8	-17.6	-38.2	-29.6	-29.2	-18.6	-20.02	...	-18.8
B3LYP/cc-pVTZ	-23.7	-47.4	-15.8	-37.4	-28.5	-26.9	-16.4	-17.56	...	-16.4
CCSD(T)/6-31G*	-28.5	-50.8	-19.0	-42.2	-32.6	-30.6	-20.1	-21.66	...	-20.3
CCSD(T)/cc-pVTZ	-28.9	-48.0	-16.5	-42.6	-31.5	-27.6	-17.3	-18.60	...	-17.3

^aaug-cc-pVTZ(C,O)+aug-cc-pVDZ(H).TABLE II. B3LYP and CCSD specific rotation [$\text{deg dm}^{-1} (\text{g/mL})^{-1}$] for (S)-methyloxirane computed with various basis sets and optimized geometries at 355 nm. The center of mass is chosen to be the gauge origin.

Geometry type	6-31G*	6-31++G**	6-311++G(2d,2p)	cc-pVDZ	cc-pVTZ	aug-cc-pVDZ	d-aug-cc-pVDZ	mixed-cc-pVTZ ^a	aug-cc-pVTZ	Sadlej-pVTZ
B3LYP (GIAO)										
B3LYP/6-31G*	-51.9	-57.2	9.36	-122	-40.4	-5.19	20.3	6.29	11.4	46.8
B3LYP/cc-pVTZ	-51.5	-56.7	14.8	-119	-36.1	2.80	27.8	14.28	19.5	57.1
CCSD(T)/6-31G*	-67.7	-61.7	4.60	-135	-49.5	-9.87	17.3	0.68	6.97	41.8
CCSD(T)/cc-pVTZ	-73.9	-61.3	12.5	-138	-46.4	-0.52	28.9	10.08	16.6	52.6
B3LYP (non-GIAO)										
B3LYP/6-31G*	-76.0	-53.2	41.7	-117	-59.1	-11.7	25.4	14.69	15.7	19.4
B3LYP/cc-pVTZ	-74.1	-46.4	47.5	-114	-54.7	-4.01	33.2	23.44	24.1	25.5
CCSD(T)/6-31G*	-90.0	-58.2	37.8	-129	-68.3	-15.9	20.9	10.23	11.2	15.1
CCSD(T)/cc-pVTZ	-90.8	-47.9	46.3	-130	-63.9	-6.54	30.3	20.86	21.6	25.3
CCSD										
B3LYP/6-31G*	-65.0	-118	-22.4	-102	-71.0	-56.8	-24.3	-32.84	...	-24.9
B3LYP/cc-pVTZ	-63.1	-110	-17.0	-98.6	-67.4	-49.9	-17.8	-25.50	...	-17.7
CCSD(T)/6-31G*	-78.5	-120	-26.2	-114	-80.1	-60.6	-28.5	-37.59	...	-29.0
CCSD(T)/cc-pVTZ	-78.5	-111	-18.6	-114	-76.4	-51.4	-20.1	-28.17	...	-20.0

^aaug-cc-pVTZ(C,O)+aug-cc-pVDZ(H).

TABLE III. CCSD specific rotation [$\text{deg dm}^{-1} (\text{g/mL})^{-1}$] for (*S*)-methyloxirane with the gauge origin placed at the center-of-mass (COM) or at the coordinates of the oxygen atom (O).

Geometry type	CCSD/aug-cc-pVDZ				CCSD/d-aug-cc-pVDZ			
	355 nm		589 nm		355 nm		589 nm	
	COM	O	COM	O	COM	O	COM	O
B3LYP/6-31G*	-56.8	-77.8	-29.2	-36.2	-24.4	-55.7	-18.6	-28.9
B3LYP/cc-pVTZ	-49.9	-69.7	-26.9	-33.5	-17.8	-47.6	-16.4	-26.2
CCSD(T)/6-31G*	-60.6	-81.5	-30.6	-37.6	-28.5	-60.1	-20.1	-30.4
CCSD(T)/cc-pVTZ	-51.4	-71.1	-27.6	-34.2	-20.0	-50.0	-17.3	-27.1

theory using a variety of basis sets at the two key wavelengths: 589 and 355 nm, respectively. Nearly all choices of basis set and optimized geometry for both methods predict a negative value of $[\alpha]_{589}$, in qualitative agreement with the CCl_4 -solvent-dependent experimental result of $-18.7 \text{ deg dm}^{-1} (\text{g/mL})^{-1}$ of Kumata *et al.*,³² though, as noted earlier, the influence of solvent may be considerable. On the other hand, the variation of the results with respect to basis set even for the GIAO-based B3LYP method, is striking. We find that the effect of diffuse functions in the basis set is particularly important, in agreement with previous studies by Cheeseman *et al.*^{6,8} and by Wiberg *et al.*²⁸ While the 6-31G*, cc-pVDZ, and cc-pVTZ basis sets, which lack diffuse functions, give values of $[\alpha]_{589}$ that are too large in magnitude, even the 6-31++G** basis set, which includes diffuse *s* and *p* functions for the heavy atoms and diffuse *s* functions on the hydrogens, produces angles around $-35 \text{ deg dm}^{-1} (\text{g/mL})^{-1}$ for B3LYP and near $-50 \text{ deg dm}^{-1} (\text{g/mL})^{-1}$ for CCSD. The aug-cc-pVDZ basis set, which also includes diffuse *d* functions on the heavy atoms and diffuse *p* functions on the hydrogens, performs well for B3LYP, but poorly for CCSD, while the d-aug-cc-pVDZ basis set, which includes two sets of diffuse functions for each atom, reverses this behavior. Finally, the Sadlej-pVTZ basis, which is optimized for computing electrical response properties, gives essentially the same CCSD $[\alpha]_{589}$ as d-aug-cc-pVDZ, but B3LYP values that are near zero (and even positive with the B3LYP/cc-pVTZ geometry).

The variation in the values of $[\alpha]_{355}$ (Table II) with respect to basis set is even greater than that of $[\alpha]_{589}$. For the basis sets lacking diffuse functions, strong negative rotation angles are computed for all methods—even greater than $100 \text{ deg dm}^{-1} (\text{g/mL})^{-1}$ for CCSD/cc-pVDZ, in dramatic disagreement with the gas-phase CRDP result of $[\alpha]_{355} = +10.2 \text{ deg dm}^{-1} (\text{g/mL})^{-1}$ of Müller and co-workers. For the larger basis sets that include diffuse functions, the B3LYP predictions of $[\alpha]_{355}$ are positive, in qualitative to semiquantitative agreement with experiment, while the CCSD results remain negative for all the basis sets used here. Furthermore, the B3LYP results show the correct direction of the dispersion in $[\alpha]_{\lambda}$ (more positive for 355 nm than for 589 nm) for several of the more diffuse basis sets, while CCSD rotation angles are consistently more negative at 355 nm than their 589 nm counterparts. In short, none of the coupled cluster calculations of $[\alpha]_{355}$ carried out in this work are in even qualitative agreement with the experimental data by Müller *et al.*

In addition, Tables I and II also reveal a surprisingly strong dependence of the computed values of $[\alpha]_{\lambda}$ on the choice of optimized geometry. Although computed values of $[\alpha]_{589}$ vary with structure by only a few $\text{deg dm}^{-1} (\text{g/mL})^{-1}$ for a given method and basis set, for the $[\alpha]_{355}$ data, the variation can be greater than $15 \text{ deg dm}^{-1} (\text{g/mL})^{-1}$, as observed for the B3LYP/Sadlej-pVTZ and CCSD/6-31G* levels of theory. This disparity occurs in spite of the rather small structural differences among the four optimized geometries shown in Fig. 1.

Optical rotation calculations were also carried out to assess the origin dependence of the CCSD results and the effect of using London orbitals/GIAOs with DFT. Tables I and II therefore include B3LYP optical rotation data both with and without GIAOs for the 355 and 589 nm wavelengths. For most basis sets, the non-GIAO B3LYP results differ little [usually less than $5 \text{ deg dm}^{-1} (\text{g/mL})^{-1}$] from their GIAO-based counterparts. Two notable exceptions are the Sadlej-pVTZ and the mixed aug-cc-pVTZ/aug-cc-pVDZ basis set results for $[\alpha]_{355}$: without GIAOs the B3LYP data shift by more than $25 \text{ deg dm}^{-1} (\text{g/mL})^{-1}$ towards the experimental result for the former and nearly $20 \text{ deg dm}^{-1} (\text{g/mL})^{-1}$ away from the experimental result for the latter. Table III reports CCSD/aug-cc-pVDZ and CCSD/d-aug-cc-pVDZ optical rotation data for 355 and 589 nm wavelengths for the four optimized structures computed at two choices of gauge origin: the molecular center-of-mass and the coordinates of the oxygen atom. In every case, the rotation becomes more negative as the origin shifts away from the center-of-mass by as much as $30 \text{ deg dm}^{-1} (\text{g/mL})^{-1}$ for the d-aug-cc-pVDZ basis set and the results are again much more sensitive for $[\alpha]_{355}$ than for $[\alpha]_{589}$.

The above results beg an important question: why does B3LYP appear to perform somewhat better for the 355 nm optical rotation than CCSD, giving rotation angles that are at least in qualitative agreement with the experimental result of Müller and co-workers? The answer lies in the ability of each method, B3LYP and CCSD, to describe the first-order pole structure (the Cotton effect) in $[\alpha]_{\lambda}$ implied by Eq. (1) as the frequency of the incident radiation approaches resonance with an electronic excitation. In CC response theory, the occurrence and shape of such a pole depends both on the structure of the perturbed wave functions, \hat{X}_{μ}^{ω} , determined in Eq. (4), and the dependence of the linear response function in Eq. (3) on these functions. The appearance of the EOM-CC response matrix, $\langle \Phi_i | (\bar{H} - \omega) | \Phi_j \rangle$ in Eq. (4) indicates that,

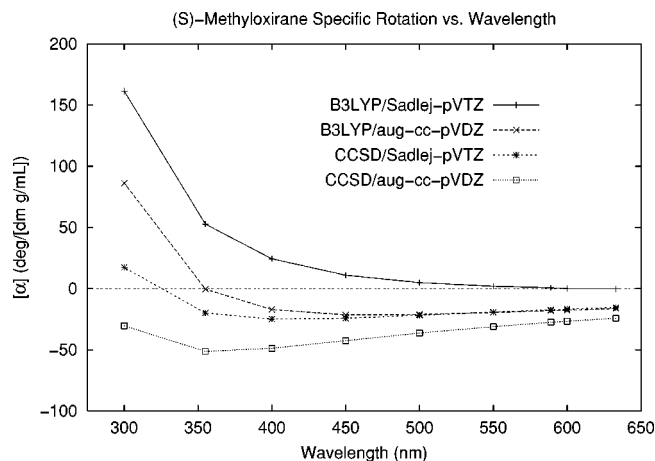


FIG. 2. Calculated optical rotary dispersion curve for (S)-2-methyloxirane using B3LYP and CCSD linear response methods with the Sadlej-pVTZ and aug-cc-pVDZ basis sets.

as ω approaches an eigenvalue of \bar{H} (an excitation energy) the perturbed wave function components will become infinitely large (with variable sign). However, as noted previously by Christiansen *et al.*,⁴⁵ although the CC-linear response function contains terms that depend *quadratically* on the perturbed wave functions (i.e., the second term on the right-hand side of Eq. (3), this does not obviate the ability of coupled cluster response theory to produce a correct first-order pole structure in $[\alpha]_{\lambda}$. (It is worth noting that this point is closely related to the ability of coupled cluster methods to describe correctly the first-order pole structure of vibrational force constants in pseudo-Jahn-Teller theory, a topic pertinent to studies of real and artifactual symmetry breaking in polyatomic molecules.⁸³⁻⁸⁵)

Density-functional response theory, on the other hand, benefits from variational optimization of the component Kohn-Sham orbitals, and a linear response function that closely resembles that of the random-phase approximation (RPA):¹⁸

$$\langle\langle \boldsymbol{\mu}; \mathbf{m} \rangle\rangle_{\omega} = (\boldsymbol{\mu}_S \quad \boldsymbol{\mu}_{S^+}) \begin{pmatrix} \mathbf{A} - \omega \mathbf{I} & \mathbf{B} \\ -\mathbf{B} & -\mathbf{A} + \omega \mathbf{I} \end{pmatrix}^{-1} \begin{pmatrix} \mathbf{m}_S \\ \mathbf{m}_{S^+} \end{pmatrix}, \quad (5)$$

TABLE IV. EOM-CCSD and B3LYP-TDDFT excitation energies for the two lowest Rydberg states of (S)-methyloxirane computed with various basis sets and optimized geometries.

Geometry type	EOM-CCSD						B3LYP/TDDFT					
	aug-cc-pVDZ		d-aug-cc-pVDZ		Sadlej-pVTZ		aug-cc-pVDZ		d-aug-cc-pVDZ		Sadlej-pVTZ	
	eV	nm	eV	nm	eV	nm	eV	nm	eV	nm	eV	nm
B3LYP/6-31G*	7.17	173	7.14	174	7.14	174	6.54	190	6.48	191	6.58	188
	7.63	162	7.38	166	7.42	167	6.98	176	6.89	180	7.03	176
B3LYP/cc-pVTZ	7.18	173	7.14	174	7.14	174	6.54	190	6.48	191	6.58	188
	7.48	166	7.39	168	7.60	163	6.99	178	6.89	180	7.03	176
CCSD(T)/6-31G*	7.16	173	7.13	174	7.13	174	6.53	190	6.48	191	6.57	189
	7.43	167	7.56	164	7.39	168	6.97	178	6.88	180	7.01	177
CCSD(T)/cc-pVTZ	7.19	172	7.15	173	7.16	173	6.55	189	6.49	191	6.59	188
	7.49	166	7.59	163	7.44	168	6.99	177	6.89	180	7.04	176

where the submatrices \mathbf{A} and \mathbf{B} represent matrix elements of the Kohn-Sham effective Hamiltonian between excited determinants, and the property vectors include single excitations (subscript S) and single deexcitations (subscript S^+). The eigenvalues of the inverted response matrix appearing in Eq. (5) represent excitation energies, but because the TDDFT linear response function depends at most linearly on the (implicit) perturbed wave functions, the method will give a correct first-order pole at resonance.

Thus, two questions remain: (1) How well do CCSD and B3LYP methods predict the *position* of the pole in $[\alpha]_{\lambda}$, i.e., the excitation energies of the system, and (2) how well do they reproduce the *shape* of the pole? Figure 2 plots the optical rotary dispersion spectrum of (S)-methyloxirane for the B3LYP/Sadlej-pVTZ, B3LYP/aug-cc-pVDZ, CCSD/Sadlej-pVTZ, and CCSD/aug-cc-pVDZ methods at the CCSD(T)/cc-pVTZ optimized geometry. As the radiation wavelength becomes shorter, all four methods predict an increase in $[\alpha]_{\lambda}$, as expected. However, the B3LYP method clearly rises more rapidly than its CCSD counterpart, in apparent agreement with the experimental data.

However, this behavior of the B3LYP linear response function stems from an *incorrect* prediction of the position of the pole. Table IV reports vertical excitation energies for the lowest two excited states of (S)-methyloxirane both of which are Rydberg transitions using TDDFT/B3LYP and the EOM-CCSD method with several different basis sets that include diffuse functions, all using the CCSD(T)/cc-pVTZ optimized geometry. The corresponding experimental excitations reported by Cohen *et al.* are 7.12 eV (174.1 nm) and 7.75 eV (160.0 nm).³⁷ As can be seen from the table, the B3LYP method is in error by 0.5–0.6 eV *too low*. (Such errors of TDDFT with current functionals are common for Rydberg-type excitations.) Thus, the position of the B3LYP pole in $[\alpha]_{\lambda}$ is shifted *closer* to the 355 nm wavelength of the incident radiation, resulting in a faster rise in the rotation angle, and apparently fortuitously agreement with the experimental result of Müller and co-workers.

On the other hand, Table IV shows that the EOM-CCSD method gives a lowest-energy excitation that is essentially identical to the experimental result (within only 0.05 eV). However, while the CCSD method clearly predicts a correct

position of the pole, the width and curvature of the pole are clearly underestimated, resulting in poor agreement with the experimental value of $[\alpha]_{355}$ experimental value.

V. CONCLUSIONS

We have presented theoretical calculations of optical rotation angles for the difficult case of (*S*)-methyloxirane using TDDFT/B3LYP and coupled cluster linear response theories. We find that both methods are exquisitely sensitive to the choice of one-electron basis set and that diffuse functions have a particularly large impact on the computed values of $[\alpha]_{\lambda}$. Furthermore, both methods show a surprising sensitivity to the choice of optimized geometry, with $[\alpha]_{355}$ values varying by as much as $15 \text{ deg dm}^{-1} (\text{g/mL})^{-1}$ among structures that appear to differ only negligibly.

At first glance, the DFT optical rotation angles appear to be superior to those of the CCSD method. For example, the B3LYP $[\alpha]_{355}$ values computed with large, diffuse basis sets agree reasonably well with the experimental gas-phase results of Müller and co-workers, while those from CCSD are qualitatively incorrect. However, the success of DFT in this case may actually stem from a cancellation of errors. Specifically, the B3LYP functional underestimates the lowest electronic excitation energy of (*S*)-methyloxirane by 0.5–0.6 eV, thus shifting the first-order pole (the Cotton effect) in $[\alpha]_{\lambda}$ towards the experimentally chosen incident radiation lines, resulting in a fortuitous positive shift in the value of $[\alpha]_{355}$ towards the experimental result. On the other hand, while the CCSD method correctly predicts the position of the pole, with a lowest excitation energy within only 0.05 eV of experiment, the shape/curvature of the ORD region near $\lambda=355 \text{ nm}$ is still significantly in error.

We agree wholeheartedly with the assessment of Giorgio *et al.*³³ that the optical rotation of (*S*)-methyloxirane is one of the most difficult cases to be treated to date. In order to eventually resolve these discrepancies between theory and experiment, we are working to extend our coupled cluster response programs in two important directions: (1) implementation of GIAOs for CC optical rotation in an effort improve the dramatic basis set dependence of the computed rotation angles; and (2) inclusion of triple excitations in the CC ansatz [e.g., the CC3 or EOM-CCSD(T) methods] to determine the importance of residual dynamic electron correlation effects. We will report on these developments in future publications.

ACKNOWLEDGMENTS

This work was supported by a National Science Foundation CAREER Award (CHE-0133174), a Cottrell Scholar Award from the Research Corporation, a New Faculty Award from the Camille and Henry Dreyfus Foundation, the Jeffress Memorial Trust, and a Lab-Directed Research and Development (LDRD) Contract with the Department of Energy through Sandia National Laboratory (Livermore). The authors thank Professor Kenneth Ruud (University of Tromsø) for helpful discussions.

- ¹E. L. Eliel and S. H. Wilen, *Stereochemistry of Organic Compounds* (Wiley, New York, 1994).
- ²E. Charney, *The Molecular Basis of Optical Activity: Optical Rotatory Dispersion and Circular Dichroism* (Wiley, New York, 1979).
- ³P. L. Polavarapu and D. K. Chakraborty, *J. Am. Chem. Soc.* **120**, 6160 (1998).
- ⁴P. L. Polavarapu and D. K. Chakraborty, *Chem. Phys. Lett.* **240**, 1 (1999).
- ⁵P. J. Stephens, F. J. Devlin, J. R. Cheeseman, M. J. Frisch, B. Mennucci, and J. Tomasi, *Tetrahedron: Asymmetry* **11**, 2443 (2000).
- ⁶J. R. Cheeseman, M. J. Frisch, F. J. Devlin, and P. J. Stephens, *J. Phys. Chem. A* **104**, 1039 (2000).
- ⁷F. Furche, R. Ahlrichs, C. Wachsmann, E. Weber, A. Sobanski, F. Vögtle, and S. Grimme, *J. Am. Chem. Soc.* **122**, 1717 (2000).
- ⁸P. J. Stephens, F. J. Devlin, J. R. Cheeseman, and M. J. Frisch, *J. Phys. Chem. A* **105**, 5356 (2001).
- ⁹P. L. Polavarapu, *Mol. Phys.* **91**, 551 (1997).
- ¹⁰L. Rosenfeld, *Z. Phys.* **52**, 161 (1928).
- ¹¹Y. H. Pao and D. P. Santry, *J. Am. Chem. Soc.* **88**, 4157 (1966).
- ¹²T. D. Bouman and D. A. Lightner, *J. Am. Chem. Soc.* **98**, 3145 (1976).
- ¹³A. Volosov, *Int. J. Quantum Chem.* **36**, 473 (1989).
- ¹⁴R. D. Amos, *Chem. Phys. Lett.* **87**, 23 (1982).
- ¹⁵T. Helgaker, K. Ruud, K. L. Bak, P. Jørgensen, and J. Olsen, *Faraday Discuss.* **99**, 165 (1994).
- ¹⁶K. Ruud, P. R. Taylor, and P.-O. Åstrand, *Chem. Phys. Lett.* **337**, 217 (2001).
- ¹⁷S. Grimme, *Chem. Phys. Lett.* **339**, 380 (2001).
- ¹⁸S. Grimme, F. Furche, and R. Ahlrichs, *Chem. Phys. Lett.* **361**, 321 (2002).
- ¹⁹K. Ruud and T. Helgaker, *Chem. Phys. Lett.* **352**, 533 (2002).
- ²⁰K. Ruud, P. J. Stephens, F. J. Devlin, P. R. Taylor, J. R. Cheeseman, and M. J. Frisch, *Chem. Phys. Lett.* **373**, 606 (2003).
- ²¹T. B. Pedersen, H. Koch, and K. Ruud, *J. Chem. Phys.* **110**, 2883 (1999).
- ²²R. K. Kondru, P. Wipf, and D. N. Beratan, *Science* **282**, 2247 (1998).
- ²³R. K. Kondru, P. Wipf, and D. N. Beratan, *J. Am. Chem. Soc.* **120**, 2204 (1998).
- ²⁴S. Ribe, R. K. Kondru, D. N. Beratan, and P. Wipf, *J. Am. Chem. Soc.* **122**, 4608 (2000).
- ²⁵T. L. Perry, A. Dickerson, A. A. Khan, R. K. Kondru, D. N. Beratan, P. Wipf, M. Kelly, and M. T. Hamann, *Tetrahedron* **57**, 1483 (2001).
- ²⁶C. Diedrich and S. Grimme, *J. Phys. Chem. A* **107**, 2524 (2003).
- ²⁷K. B. Wiberg, P. H. Vaccaro, and J. R. Cheeseman, *J. Am. Chem. Soc.* **125**, 1888 (2003).
- ²⁸K. B. Wiberg, Y. G. Wang, P. H. Vaccaro, J. R. Cheeseman, G. Trucks, and M. J. Frisch, *J. Phys. Chem. A* **108**, 32 (2004).
- ²⁹B. C. Rinderspacher and P. R. Schreiner, *J. Phys. Chem. A* **108**, 2867 (2004).
- ³⁰T. Müller, K. B. Wiberg, P. H. Vaccaro, J. R. Cheeseman, and M. J. Frisch, *J. Opt. Soc. Am. B* **19**, 125 (2002).
- ³¹T. Müller, K. B. Wiberg, and P. H. Vaccaro, *J. Phys. Chem. A* **104**, 5959 (2000).
- ³²Y. Kumata, J. Furukawa, and T. Fueno, *Bull. Chem. Soc. Jpn.* **43**, 3920 (1970).
- ³³E. Giorgio, C. Rosini, R. G. Viglione, and R. Zanasi, *Chem. Phys. Lett.* **376**, 452 (2003).
- ³⁴T. H. Dunning, *J. Chem. Phys.* **90**, 1007 (1989).
- ³⁵A. J. Sadlej, *Coll. Czech. Chem. Commun.* **53**, 1995 (1988).
- ³⁶A. J. Sadlej, *Theor. Chim. Acta* **79**, 123 (1991).
- ³⁷D. Cohen, M. Levi, H. Basch, and A. Gedanken, *J. Am. Chem. Soc.* **105**, 1738 (1983).
- ³⁸T. D. Crawford and H. F. Schaefer, in *Reviews in Computational Chemistry*, edited by K. B. Lipkowitz and D. B. Boyd (VCH, New York, 2000), Vol. 14, Chap. 2, pp. 33–136.
- ³⁹R. J. Bartlett, in *Modern Electronic Structure Theory*, Vol. 2 of *Advanced Series in Physical Chemistry*, edited by D. R. Yarkony (World Scientific, Singapore, 1995), Chap. 16, pp. 1047–1131.
- ⁴⁰T. J. Lee and G. E. Scuseria, in *Quantum Mechanical Electronic Structure Calculations with Chemical Accuracy*, edited by S. R. Langhoff (Kluwer Academic, Dordrecht, 1995), pp. 47–108.
- ⁴¹J. Gauss, in *Encyclopedia of Computational Chemistry*, edited by P. Schleyer (Wiley, New York, 1998).
- ⁴²H. J. Monkhorst, *Int. J. Quantum Chem., Symp.* **11**, 421 (1977).
- ⁴³H. Koch and P. Jørgensen, *J. Chem. Phys.* **93**, 3333 (1990).
- ⁴⁴J. Olsen and P. Jørgensen; in *Modern Electronic Structure Theory*, Vol. 2

- of *Advanced Series in Physical Chemistry*, edited by D. Yarkony (World Scientific, Singapore, 1995), Chap. 13, pp. 857–990.
- ⁴⁵O. Christiansen, P. Jørgensen, and C. Hättig, *Int. J. Quantum Chem.* **68**, 1 (1998).
- ⁴⁶O. Christiansen, A. Halkier, H. Koch, P. Jørgensen, and T. Helgaker, *J. Chem. Phys.* **108**, 2801 (1998).
- ⁴⁷L. Adamowicz, W. D. Laidig, and R. J. Bartlett, *Int. J. Quantum Chem., Quantum Chem. Symp.* **18**, 245 (1984).
- ⁴⁸G. Fitzgerald, R. Harrison, W. D. Laidig, and R. J. Bartlett, *Chem. Phys. Lett.* **117**, 433 (1985).
- ⁴⁹R. J. Bartlett, in *Geometrical Derivatives of Energy Surfaces and Molecular Properties*, edited by P. Jørgensen and J. Simons (Reidel, Dordrecht, 1986), pp. 35–61.
- ⁵⁰A. C. Scheiner, G. E. Scuseria, J. E. Rice, T. J. Lee, and H. F. Schaefer, *J. Chem. Phys.* **87**, 5361 (1987).
- ⁵¹J. Gauss, W. J. Lauderdale, J. F. Stanton, J. D. Watts, and R. J. Bartlett, *Chem. Phys. Lett.* **182**, 207 (1991).
- ⁵²J. F. Stanton and R. J. Bartlett, *J. Chem. Phys.* **98**, 7029 (1993).
- ⁵³G. D. Purvis and R. J. Bartlett, *J. Chem. Phys.* **76**, 1910 (1982).
- ⁵⁴M. Rittby and R. J. Bartlett, *J. Phys. Chem.* **92**, 3033 (1988).
- ⁵⁵T. D. Crawford, C. D. Sherrill, E. F. Valeev, J. T. Fermann, R. A. King, M. L. Leininger, S. T. Brown, C. L. Janssen, E. T. Seidl, J. P. Kenny, and W. D. Allen, *PSI 3.2* (2003).
- ⁵⁶J. F. Stanton, J. Gauss, J. D. Watts, and R. J. Bartlett, *J. Chem. Phys.* **94**, 4334 (1991).
- ⁵⁷J. Gauss, J. F. Stanton, and R. J. Bartlett, *J. Chem. Phys.* **95**, 2623 (1991).
- ⁵⁸T. B. Pedersen and H. Koch, *Chem. Phys. Lett.* **293**, 251 (1998).
- ⁵⁹T. B. Pedersen, H. Koch, and C. Hättig, *J. Chem. Phys.* **110**, 8318 (1999).
- ⁶⁰T. B. Pedersen, B. Fernández, and H. Koch, *J. Chem. Phys.* **114**, 6983 (2001).
- ⁶¹F. London, *J. Phys. Radium* **8**, 397 (1937).
- ⁶²R. Ditchfield, *Mol. Phys.* **27**, 789 (1974).
- ⁶³T. Helgaker and P. Jørgensen, *J. Chem. Phys.* **95**, 2595 (1991).
- ⁶⁴T. Helgaker and P. R. Taylor, in *Modern Electronic Structure Theory*, Vol. 2 of *Advanced Series in Physical Chemistry*, edited by D. Yarkony (World Scientific, Singapore, 1995), Chap. 12, pp. 725–856.
- ⁶⁵R. G. Parr and W. Yang, *Density-Functional Theory of Atoms and Molecules* (Oxford University Press, New York, 1989).
- ⁶⁶C. Lee, W. Yang, and R. G. Parr, *Phys. Rev. B* **37**, 785 (1988).
- ⁶⁷A. D. Becke, *J. Chem. Phys.* **98**, 5648 (1993).
- ⁶⁸K. Raghavachari, G. W. Trucks, J. A. Pople, and M. Head-Gordon, *Chem. Phys. Lett.* **157**, 479 (1989).
- ⁶⁹R. J. Bartlett, J. D. Watts, S. A. Kucharski, and J. Noga, *Chem. Phys. Lett.* **165**, 513 (1990); Erratum **167**, 609 (1990).
- ⁷⁰T. J. Lee and A. P. Rendell, *J. Chem. Phys.* **94**, 6229 (1991).
- ⁷¹G. E. Scuseria, *J. Chem. Phys.* **94**, 442 (1991).
- ⁷²P. C. Hariharan and J. A. Pople, *Theor. Chim. Acta* **28**, 213 (1973).
- ⁷³J. F. Stanton and J. Gauss, in *Recent Advances in Coupled-Cluster Methods*, edited by R. J. Bartlett (World Scientific, Singapore, 1997), pp. 49–79.
- ⁷⁴J. Gauss and J. F. Stanton, *Chem. Phys. Lett.* **276**, 70 (1997).
- ⁷⁵C. Jamorski, M. E. Casida, and D. R. Salahub, *J. Chem. Phys.* **104**, 5134 (1996).
- ⁷⁶R. Bauernschmitt and R. Ahlrichs, *Chem. Phys. Lett.* **256**, 454 (1996).
- ⁷⁷R. A. Kendall, T. H. Dunning, and R. J. Harrison, *J. Chem. Phys.* **96**, 6796 (1992).
- ⁷⁸D. E. Woon and T. H. Dunning, *J. Chem. Phys.* **100**, 2975 (1994).
- ⁷⁹Basis sets were obtained from the Extensible Computational Chemistry Environment Basis Set Database, Version 12/03/03, as developed and distributed by the Molecular Science Computing Facility, Environmental and Molecular Sciences Laboratory which is part of the Pacific Northwest Laboratory, P.O. Box 999, Richland, WA 99352, USA, and funded by the U.S. Department of Energy. The Pacific Northwest Laboratory is a multi-program laboratory operated by Battelle Memorial Institute for the U.S. Department of Energy under Contract No. DE-AC06-76RLO 1830. Contact D. Feller or K. Schuchardt for further information.
- ⁸⁰M. J. Frisch *et al.*, GAUSSIAN 03, Gaussian, Inc., Pittsburgh, PA, 2003.
- ⁸¹J. F. Stanton, J. Gauss, J. D. Watts, W. J. Lauderdale, and R. J. Bartlett, ACES II, 1993. The package also contains modified versions of the MOLECULE Gaussian integral program of J. Almlöf and P. R. Taylor, the ABACUS integral derivative program written by T. U. Helgaker, H. J. Aa. Jensen, P. Jørgensen, and P. R. Taylor, and the PROPS property evaluation integral code of P. R. Taylor.
- ⁸²R. A. Creswell and R. H. Schwendeman, *J. Mol. Spectrosc.* **64**, 295 (1977).
- ⁸³T. D. Crawford, J. F. Stanton, W. D. Allen, and H. F. Schaefer, *J. Chem. Phys.* **107**, 10626 (1997).
- ⁸⁴J. F. Stanton, *J. Chem. Phys.* **115**, 10382 (2001).
- ⁸⁵N. J. Russ and T. D. Crawford, *J. Chem. Phys.* **120**, 7298 (2004).